Ligand-Dependent Inhibition and Reversal of Tau Filament Formation†

Carmen Chirita,‡,§ Mihaela Necula,‡,§ and Jeff Kuret*,‖

Biophysics Program and Department of Molecular and Cellular Biochemistry, The Ohio State University College of Medicine and Public Health, Columbus, Ohio 43210

Received November 21, 2003; Revised Manuscript Received January 12, 2004

ABSTRACT: Alzheimer's disease is defined in part by the intraneuronal accumulation of filaments comprised of the microtubule associated protein tau. Because animal model studies suggest that a toxic gain of function accompanies tau aggregation in neurons, selective pharmacological inhibitors of the process may have utility in slowing neurodegeneration. Here, the properties of a candidate small molecule inhibitor of tau fibrillization, 3-(2-hydroxyethyl)-2-[2-[[3-(2-hydroxyethyl)-5-methoxy-2-benzothiazolylidene]methyl]-1-butenyl]-5-methoxybenzothiazolium (N744), were characterized in vitro using transmission electron microscopy. N744 inhibited arachidonic acid-induced aggregation of full-length, four-repeat tau protein at substoichiometric concentrations relative to total tau and with an IC_{50} of ~300 nM. Inhibition was accompanied by a dose-dependent decrease in the number concentration of filaments, suggesting that N744 interfered with tau filament nucleation. Stoichiometric concentrations of N744 also promoted tau disaggregation when added to mature synthetic filaments. Disaggregation followed first-order kinetics and was accompanied by a steady decrease in filament number, suggesting that N744 promoted endwise loss of tau molecules with limited filament breakage. N744 at substoichiometric concentrations did not inhibit Aβ and α-synuclein aggregation, indicating it was tau selective under these conditions. Because of its activity in vitro, N744 may offer a pharmacological approach to the role of tau fibrillization in neurodegeneration.

Neuritic plaques, neurofibrillary tangles, and neuropil threads are hallmark lesions of Alzheimer's disease (AD)[1] that contain filamentous intraneuronal inclusions of tau protein (*1*). Because tau filaments form in brain regions associated with memory retention, and because their appearance correlates well with the degree of dementia, they have emerged as robust markers of disease progression (*2*, *3*). Tau filaments also appear in other neurodegenerative tauopathies, including Pick's disease and corticobasal degeneration, with the neuronal populations affected being disease dependent (*4*). Thus, tau filament formation heralds the onset of cytoskeletal disorganization that is characteristic of degenerating neurons and may represent a fundamental pathobiological response of neurons to various insults.

Genetic studies have extended these observations by establishing a direct link between certain neurodegenerative disorders and mutations in the tau gene (*5*). These autosomal-dominant dementias, such as FTDP-17, fall into several classes. One class consists of point mutations within the coding sequence of tau protein. A second class consists of intronic mutations that affect the distribution of alternatively spliced tau isoforms found in the insoluble tau deposits of these disorders. Each of the resultant tauopathies accumulates filamentous tau inclusions (*5*), as do transgenic mice harboring the P301L FTDP-17 mutation (*6*, *7*). These findings emphasize the importance of tau protein in normal neuronal function and show that changes in tau structure can lead directly to filament formation and neurodegeneration.

In fact, merely overexpressing human tau in lamprey reticulospinal neurons is sufficient to drive filament accumulation and subsequent neuronal death (*8*, *9*). In the lamprey system, neurons continue to function until a critical mass of tau filaments is present. Overexpression of other polymerizing proteins, such as the neurofilament protomer NF180, also leads to filament formation but not neurodegeneration (*10*). These data suggest that the assembly of tau protein into filamentous forms leads to a toxic gain of function for tau that exacerbates or potentially mediates degeneration in affected neurons.

Confirming these findings in vitro has been challenging because purified recombinant tau preparations do not aggregate spontaneously at physiological concentrations (low micromolar) and temperatures (*11*). However, efficient formation of tau filaments with straight morphology from full-length tau protein can be induced in a matter of hours by the addition of fatty acids at 50−100 μM concentration (*11*, *12*). These agents act by forming micelles that present a negatively charged surface to the tau protein (*13*, *14*). Fatty acid-induced synthetic straight filaments are closely related to paired helical filaments found in AD and appear to

† This work was supported by National Institute of Health Grant AG14452 (J.K.).

* To whom correspondence should be addressed. E-mail: kuret.3@osu.edu. Phone: (614) 688-5899. Fax: (614) 292-5379.

‡ Biophysics Program.

§ These authors contributed equally to this work.

‖ Department of Molecular and Cellular Biochemistry.

[1] Abbreviations: Aβ, amyloid β peptide; AD, Alzheimer's disease; DMSO, dimethyl sulfoxide; FTDP-17, frontal-temporal dementia with Parkinsonism linked to chromosome 17; N744, 3-(2-hydroxyethyl)-2-[2-[[3-(2-hydroxyethyl)-5-methoxy-2-benzothiazolylidene]methyl]-1-butenyl]-5-methoxybenzothiazolium; PHF, paired-helical filament.

10.1021/bi036094h CCC: $27.50
Published on Web 02/11/2004

correspond to a single hemifilament (*11*). Over long periods of incubation (days), straight filaments adopt paired helical morphology, which is the principal form seen in late stage Alzheimer's disease (*11*, *15*). Using this paradigm, we have shown that the rate and extent of tau aggregation is influenced by C-terminal truncation and by point mutations at known FTDP-17 sites such as P301L (*16*, *17*). Thus, some of the tau modifications or mutations associated with filament formation and disease accelerate tau aggregation in vitro.

Both synthetic and authentic tau filaments adopt cross-beta sheet conformation typical of an amyloid (*18*), and on the basis of ligand-mediated assembly reactions conducted in vitro with both fragmentary and full-length tau protein, fibrillization is mediated by short hydrophobic sequences located in the microtubule repeat region (*19*). But the pathway through which the natively unfolded tau protein adopts beta-sheet structure in vivo is not clear. In vitro, evidence from the fatty-acid mediated aggregation pathway suggests that tau fibrillization is preceded by formation of an intermediate that can be bound by thioflavin S, a noncovalent probe of beta-sheet structure (*20*). Thus, it has been suggested that the intermediate may present a tractable ligand binding site for modulating tau fibrillization (*20*).

Antagonism of tau aggregation by small ligands (phenothiazines) has been demonstrated in vitro, although it was not shown that the tau aggregates inhibited were fibrillar (*21*). High concentrations (~30 mM) of some phenothiazines do disaggregate isolated authentic tau filaments, however, with extensive fragmentation (*21*). Because filament fragmentation in the presence of tau monomer can provide seeds for increased fibrillization over time, these agents may have limited utility for modulating tau filament formation in cellular and animal models.

Here, we extend the characterization of synthetic tau filaments by examining their susceptibility to pharmacological manipulation. The data show that tau fibrillization can be inhibited by a small ligand (<700 Da) acting at substoichiometric concentrations relative to tau protomer and in the presence of >100-fold molar excess of fatty acid inducer. These data support the feasibility of antagonizing and potentially reversing tau filament formation in vivo.

EXPERIMENTAL PROCEDURES

Materials. Recombinant polyhistidine-tagged htau40, htau23, and α-synuclein were expressed and purified as described previously (*22*−*24*). Human Aβ_{1-40} (Bachem; Philadelphia, PA) was dissolved in DMSO (500 μM stock), sonicated (30 min at room temperature), and filtered (0.2 μm cutoff) before use. Arachidonic acid (Fluka; Milwaukee, WI) was dissolved in 100% ethanol and stored under argon gas at −80 °C until used. Carboxylate conjugated polystyrene microspheres of defined nominal diameter and molecular area (a measure of surface charge density reported in units of Å^2/eq) were obtained from Bangs Laboratories, Inc (Fishers, IN).

Tau aggregation inhibitor 3-(2-hydroxyethyl)-2-[2-[[3-(2-hydroxyethyl)-5-methoxy-2-benzothiazolylidene]methyl]-1-butenyl]-5-methoxybenzothiazolium (Neuronautics, Inc.; Evanston, IL) was dissolved in DMSO (10 mM stock) and stored at −20 °C.

Tau Aggregation. Reactions were performed as described previously (*11*, *12*, *23*). Under standard conditions, 4−8 μM (final concentration) htau40 or htau23 was incubated with arachidonic acid or carboxylate modified polystyrene beads in assembly buffer (10 mM 4-[2-hydroxyethyl]-1-piperazineethanesulfonic acid, 100 mM NaCl, and 5 mM DTT) at 37 °C. Aggregation was induced by the addition of arachidonic acid (75−100 μM) and continued until analyzed by electron microscopy as described next. When present, the N744 final concentration was varied between 0.12 and 4.1 μM. Control reactions were normalized for the DMSO vehicle, which was limited to no more than 5% (v/v) in all aggregation reactions.

Tau Disaggregation. Solutions of purified htau40 (4 μM) were aggregated at room temperature under standard conditions as described previously for 3.5 h, then divided into two separate tubes. One tube received N744 at a final concentration of 4.7 μM, whereas the second tube received DMSO vehicle alone. Aliquots were removed from each sample after 0, 1, 3, 5, 9, 12, and 19 h incubation and subjected to the electron microscopy assay described next. Control (no N744) reactions were normalized for the DMSO vehicle, which was kept below 5.7% (v/v) in all disaggregation reactions.

Transmission Electron Microscopy. Aliquots (50 μL) of aggregation and disaggregation reactions were removed, fixed with glutaraldehyde (2%), and adsorbed (1 min) onto 300 mesh Formvar/carbon-coated copper grids (Electron Microscopy Sciences; Ft. Washington, PA). The resultant grids were washed with water, stained (1 min) with 2% uranyl acetate (Electron Microscopy Sciences), washed again with water, blotted dry, and viewed in a Phillips CM 12 microscope operated at 65 kV. Four to five random images from each experimental condition were captured on film at 22 000× magnification, digitized, calibrated, and imported into Optimas 6.5.1 for quantitation of filament length and number as described previously (*23*). Individual filaments defined as any object greater than 50 nm in its long axis were counted manually. Filament counts are reported as an average ± standard deviation for both total filament length and total filament number. Length distributions were quantified in 25 nm (assembly) or 50 nm (disassembly) wide bins.

Aβ_{1-40} and α-synuclein Aggregation. Aggregation was initiated by diluting the Aβ stock solution to 20 μM final concentration in aggregation buffer (150 mM NaCl, 10 mM 2-[*N*-morpholino]ethanesulfonic acid, pH 6.2; final volume 300 μL). Turbidity resulting from Aβ aggregation in the presence (4.1 μM final concentration) and absence of N744 was monitored as a function of time in a Beckman DU640B spectrophotometer at 400 nm versus a DMSO vehicle blank (*25*, *26*). Cuvettes were vortexed before each reading. Total DMSO vehicle concentration was controlled among samples and did not exceed 6% (v/v). Timecourse data was fit to an integral logistic equation from which the half-time to maximum absorbance, t_{50}, and the apparent rate constant for fibril growth, k_{app}, were derived (*27*). The lag time was calculated as $t_{50} - 2\tau$, where $\tau = 1/k_{app}$ (*24*).

α-Synuclein aggregation was induced at 37 °C in assembly buffer by the addition of arachidonic acid (100 μM) as described previously (*24*) and viewed by electron microscopy as described above. When N744 was present, total DMSO vehicle concentration did not exceed 5% (v/v).

Analytical Methods. Tau protein concentrations were determined by absorbance at 280 nm (*22*). Filament length

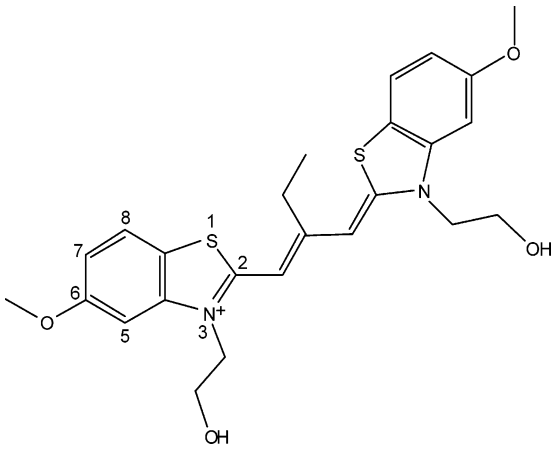

FIGURE 1: N744 structure. N744 is a cyanine derivative broadly related to the Congo Red family of dyes in that it is planar and consists of two aromatic rings flanking a hydrocarbon linker. It is predicted to be positively charged at physiological pH.

distributions were fit to the exponential equation:

$$y = ae^{bx}$$

where y is the percentage of all filaments filling a bin of length interval x, and b is a constant reported in units of length^{-1} ±SE.

All errors derived from linear regression analysis are 95% confidence limits unless otherwise noted.

RESULTS

Inhibition of Tau Fibrillization. A library of small molecules was screened for inhibitory activity against htau40 (2 μM) assembly induced by arachidonic acid (50 μM) under near-physiological conditions using a fluorescence-based assay (*12*). The structure of N744, an inhibitor identified by the screen, is shown in Figure 1. It is a charged molecule (at physiological pH) broadly related to the Congo Red family of compounds in being a planar aromatic dye.

The ability of N744 to antagonize the fibrillization of htau40 (4 μM) induced by arachidonic acid (75 μM) under standard conditions was examined by transmission electron microscopy (*11*). In the presence of DMSO vehicle alone, htau40 aggregated to form large numbers of filaments with straight morphology (Figure 2A). These appeared identical to reaction products formed in the absence of DMSO (*11*, *13*) except they were shorter (see below for quantitation). In the presence of increasing concentrations of N744 up to 4.1 μM (i.e., ≈1:1 molar stoichiometry with respect to tau protomer), however, aggregation as reflected in either the total number or total length of all filaments was greatly inhibited (Figure 2B−E). Inhibition did not derive from direct interference with arachidonic acid micellization because its CMC (measured in the presence 4 μM tau) was not significantly different in the presence and absence of 4 μM N744 (7.9 ± 2.1 and 8.1 ± 0.2 μM, respectively). Nor did it derive from interference with filament adsorption onto grids when tested at concentrations up to 50 μM (data not shown). Quantification of filament lengths revealed that N744 inhibitory activity was graded, with filament formation as measured by total filament length inhibited with an IC_{50} of 294 ± 23 nM and a Hill slope of 1.84 ± 0.14 (Figure 3). These data confirmed that N744 was a potent inhibitor of tau aggregation, being active at substoichiometric concentrations relative to total tau protomer and arachidonic acid inducer.

Isoform and Inducer Selectivity. Anionic surfactants induce tau fibrillization by forming micelles that serve as sites for filament nucleation (*13*). The pathway is mediated by an assembly intermediate that forms on the micelle surface (*20*). To determine whether N744 could inhibit fibrillization of tau induced by agents other than arachidonic acid, htau40 was incubated with anionic microspheres in the presence and absence of N744. These inducers mimic arachidonic acid by presenting a negatively charged surface on which tau can aggregate (*20*). Moreover, they facilitate visualization of surface events by virtue of their large size relative to surfactant micelles. Filaments formed from carboxylated polystyrene microspheres (90 nm diameter, 12 Å^2/eq molecular area) in DMSO vehicle alone have the same straight morphology as arachidonic acid-induced filaments, but achieve longer lengths owing to the presence of fewer nucleation sites (Figure 4A). In contrast, the presence of N744 at 4 μM (stoichiometric with total tau protein) inhibited tau fibrillization almost completely (Figure 4B). To determine whether these results were tau isoform specific, the experiment was repeated using htau23, a tau isoform containing only three microtubule binding repeats and devoid of residues encoded by exons 2 and 3 (*28*). This form nucleates less efficiently than htau40 when examined under the conditions used here (*23*). In the presence of DMSO vehicle alone, 8 μM htau23 formed microsphere-associated filaments morphologically similar to htau40 (Figure 4C). Again, N744 inhibited fibrilization almost completely (Figure 4D). These data show that N744 can inhibit fibrillization of tau isoforms containing three or four repeats and regardless of whether segments encoded by N-terminal exons two and three are present. Moreover, inhibition is not specific to arachidonic acid as fibrillization inducer.

Inhibitory Mechanism. Tau fibrillization is characterized by nucleation and extension phases. To distinguish the effect of N744 on these two phases, filament length distributions were measured as a function of inhibitor concentration and compared to control reactions containing DMSO vehicle alone. The large number of filaments formed in the control reaction adopted an exponential length distribution (Figure 5) with slope parameter (b) of -16.8 ± 0.6 μm^{-1}, which was 3.2-fold steeper (i.e., filament lengths were shorter) than control reactions prepared in the absence of DMSO ($b = -5.4 \pm 0.2$ μm^{-1}; Figure 1 in ref *13*). These data show that DMSO vehicle alone has an inhibitory effect on tau fibrillization and confirms the importance of controlling all assays for its presence. Exponential distributions were obtained at all N744 concentrations as well, but the number of filaments formed progressively decreased relative to the control reaction (Figure 5A). Because the filament number is proportional to the nucleation rate, these data suggested that one mechanism underlying N744 activity was inhibition of filament nucleation. Indeed, the dose response curves for inhibition of tau filament number and total filament length were nearly identical (Figure 3). Moreover, the slope of the length distribution decreased modestly at low concentrations of N744, consistent with fewer filaments achieving longer lengths (Figure 5B). At higher concentrations of N744, however, the pattern reversed itself with exponential distribu-

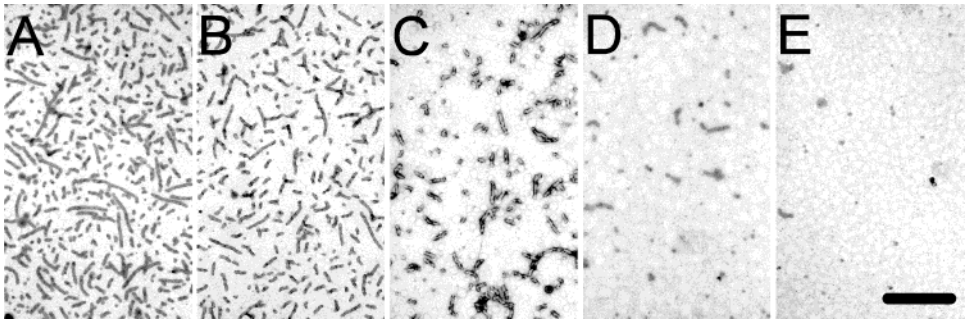

FIGURE 2: N744 is an inhibitor of tau aggregation. Htau40 (4 μM) was incubated with arachidonic acid (75 μM) and various concentrations of N744 in DMSO without agitation for 3 h at 37 °C. Aliquots were then stained with uranyl acetate and viewed in a transmission electron microscope as described in Experimental Procedures. (A) In the presence of DMSO vehicle control, htau40 formed abundant filaments. In contrast, tau fibrillization was inhibited by the presence of N744 when present at 0.12, 0.41, 1.2, and 4.1 μM (panels B−E, respectively). Bar = 500 nm.

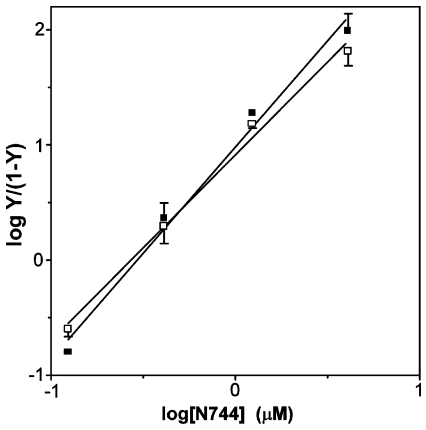

FIGURE 3: N744 inhibits tau aggregation at substoichiometric concentrations. Htau40 (4 μM) was incubated (3 h at 37 °C) with arachidonic acid (75 μM) in the presence of varying concentrations (0, 0.12, 0.41, 1.2, and 4.1 μM) of N744. Aliquots were then examined by transmission electron microscopy at 22 000-fold magnification. All filaments ≥50 nm in length were measured, summed, and plotted as total filament length (■) and total filament number (□) vs N744 concentration in Hill plot format, where Y = % control total filament length or total filament number. Each line represents linear regression analysis of data points. Both total filament length and total filament number decreased in the presence of N744, with IC_{50} values of 294 ± 23 and 272 ± 17 nM, respectively. Both Hill plots had a positive slope, with values of 1.84 ± 0.14 and 1.61 ± 0.10, respectively.

tions becoming skewed toward shorter lengths (Figure 5B). These data suggested that in addition to its effects on filament nucleation, increasing concentrations of N744 also modulated the apparent rate of tau addition to filament ends (elongation) relative to the rate of tau dissociation.

N744 Promotes Tau Filament Disaggregation. Filament elongation proceeds when the rate of addition of tau to filament ends exceeds the rate of tau protomer dissociation. If N744 decreased filament elongation relative to tau protomer dissociation, it would be predicted to disrupt the equilibrium between filamentous and nonfilamentous tau resulting in destabilization of mature synthetic filaments. To test this hypothesis, htau40 (4 μM) was fibrillized with arachidonic acid (75 μM) over a 3.5 h period after which time equal aliquots were treated with N744 (4.7 μM) or DMSO vehicle alone, and filament numbers and lengths were measured over a 19 h chase by electron microscopy. In the absence of N744, total htau40 filament length decreased 23 ± 4% over this time period (Figure 6). Because samples were diluted only 6% in the experimental paradigm, it appeared that DMSO alone destabilized tau filaments at these concentrations. In contrast, the addition of N744 (4.7 μM) led to a more rapid decrease in total filament length so that 89 ± 13% of total filament length was lost over the 19 h time course. The initial rate of filament loss was well modeled as a first-order decay (r^2 = 0.981; k = 0.12 ± 0.01 h^{-1}) under these conditions (Figure 6). These data suggested that N744 could destabilize mature filaments and decrease total filament length with first-order kinetics at a net rate (i.e., the rate corrected for dilution and DMSO effect) of 0.10 ± 0.02 h^{-1}.

Mechanism of Disaggregation. N744-mediated filament dissaggregation may result from random filament breakage or ordered disassembly from filament ends (*29*). The kinetic characteristics of endwise disaggregation of linear protein assemblies at equilibrium depend on the distribution of filament lengths (*30*). For tau filaments, which adopt an exponential distribution of lengths (*31*, *32*), dissociation rates were predicted to be first order (*30*). Moreover, filament disassembly was predicted to proceed while maintaining an exponential distribution of gradually shortening filaments lengths (*30*). This latter characteristic can distinguish endwise dissagregation from filament shearing, which can produce exponential filament lengths (*33*) while increasing filament numbers (*34*).

The observation of first-order ligand-induced filament disaggregation suggested that N744 promoted sequential release of tau protomers from filament ends instead of random filament breakage. To confirm this hypothesis, the length distribution of tau polymers were examined as function of time (19 h) after treatment of preassembled tau filaments with N744 (4.7 μM) or DMSO vehicle alone. At time 0, both N744-treated and control reactions showed distributions of tau filament lengths that were nearly identical to each other (b = −5.5 ± 0.4 and −5.3 ± 0.4 μm^{-1}, respectively; Figure 7) and to previous experimentation conducted in the absence of DMSO (b = −5.4 ± 0.2 μm^{-1}; Figure 1 in ref *13*). Consistent with the endwise disaggregation model, exponential filament length distributions were maintained throughout the N744-mediated disaggregation reaction (b = −6.1 ± 0.9 and −6.1 ± 0.4 μm^{-1} after 19 h incubation for DMSO control and N744-treated samples, respectively) as the filaments shifted to shorter lengths relative to the control reaction (shown for time 0 and 19 h only; Figure 7). Moreover, N744-mediated disaggregation was accompanied by a slow decrease in the number of

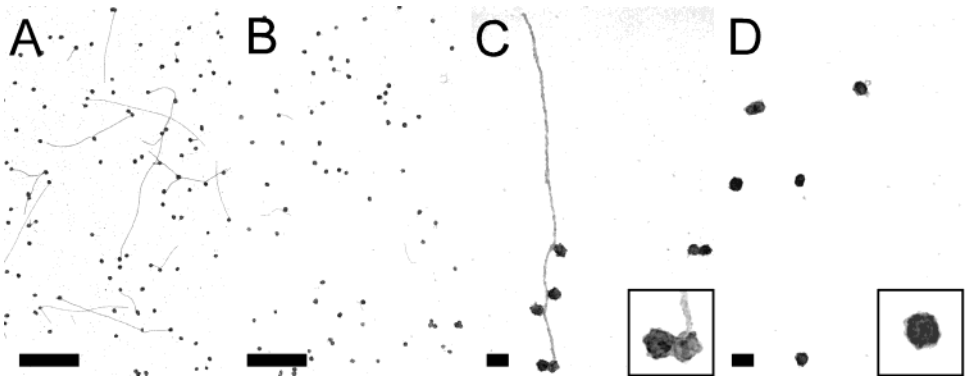

FIGURE 4: N744 inhibits microsphere-mediated tau fibrillization. Carboxylate-substituted polystyrene microspheres (90 nm diameter, 12 Å^2/eq molecular area) were incubated (37 °C) with (A and B) 4 μM htau40 (124 pM microspheres) for 6 h, or (C and D) 8 μM htau23 (276 pM microspheres) for 25 h, in the presence of DMSO vehicle (A and C) or 4 μM N744 (B and D). Aliquots were then visualized by negative stain electron microscopy. In the absence of N744, both tau preparations formed filaments extending from the microsphere surface. In contrast, the presence of N744 greatly decreased filament formation. Insets, high magnification images show that N744 blocks filament formation at the microsphere surface. Bars = (A and B) 1 μm and (C and D) 100 nm. Inset boxes = 150 nm wide.

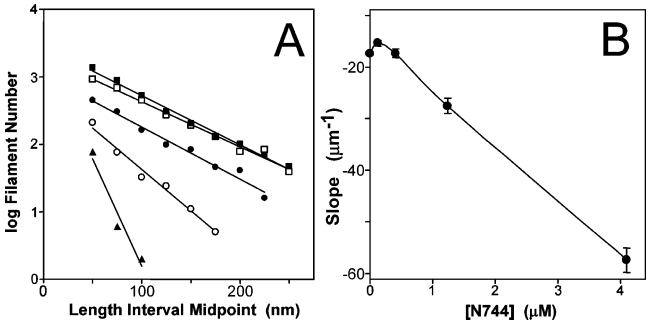

FIGURE 5: N744 inhibits both tau filament number and length. Htau40 (4 μM) was incubated (3 h) in the presence of 0 (DMSO vehicle only; ■), 0.12 (□), 0.41 (●), 1.2 (○), and 4.1 (▲) μM N744 and then examined by transmission electron microscopy at 22 000-fold magnification. Lengths and numbers of filaments ≥50 nm in length were then measured from digitized images, summed, and plotted over 4 log units. (A) Each data point represents the number of all filaments analyzed in 5 negatives (containing 3722, 2972, 1248, 379, and 92 individually measured filaments, respectively) that segregated into consecutive length intervals (25 nm bins), whereas each line represents the best fit of the data points to an exponential distribution. (B) The slope ±SE of each length distribution shown in panel A was plotted against N744 concentration. At low concentrations of N744 (≤0.41 μM), length distributions increased modestly relative to DMSO vehicle control, consistent with an effect of N744 on filament nucleation under these conditions. In contrast, further elevations of N744 concentrations (≥1.2 μM) led to significant shortening of length distributions, suggesting that inhibition of filament elongation contributed to the observed distributions.

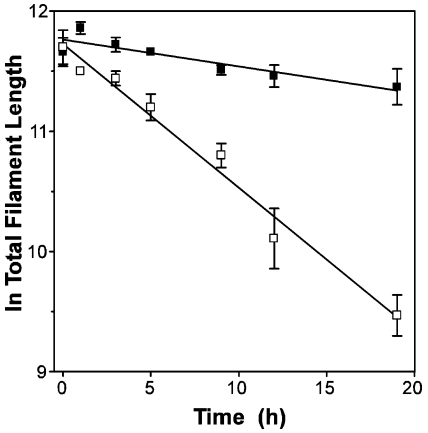

FIGURE 6: Timecourse of N744-mediated disaggregation. Filaments prepared (3.5 h at room temperature) from htau40 (4 μM) and arachidonic acid (75 μM) were split into two equal pools and further incubated in the presence of DMSO vehicle alone (■) or 4.7 μM N744 (□) for 19 h. Aliquots of each reaction were stopped at 0, 1, 3, 5, 9, 12, and 19 h by the addition of glutaraldehyde, and filaments ≥50 nm in length were analyzed by the quantitative electron microscopy assay. Each data point represents total filament length per field ± standard deviation (n = 4 observations). In the presence of DMSO vehicle alone, total tau filament length decreases slowly over time with a first-order rate of 0.022 ± 0.005 h^{-1}. In the presence of N744, however, total filament length per field decreased with an initial first-order rate of 0.12 ± 0.01 h^{-1} and a net rate of 0.10 ± 0.02 h^{-1} when corrected for DMSO vehicle alone. After 19 h incubation in the presence of 4.7 μM N744, total filament length had decreased to 13 ± 2% of that observed in vehicle only control.

filaments >50 nm in length (shown for time 0 and 19 h only; Figure 7), which was inconsistent with the random breakage-mediated disaggregation model. Together, these data suggest that N744 destabilizes tau filaments by promoting endwise filament disaggregation.

N744 Selectivity. Dyes structurally similar to N744 bind a variety of amyloid fibrils at low micromolar concentrations, including those formed from Aβ and α-synuclein (*35*). Therefore, to assess inhibitory selectivity, the aggregation of Aβ_{1-40} was followed by turbidity measurements over a period of 6 h in the presence and absence of 4 μM N744 at room temperature without agitation. Both assembly reactions followed nucleation-dependent kinetics, consisting of a slow nucleation phase characterized by a pronounced lag time, followed by an exponential growth phase characterized by an apparent first-order rate of extension, k_{app}, and then an equilibrium phase where further filament growth ceased (Figure 8A). In the absence of N744, Aβ_{1-40} (20 μM) polymerized spontaneously with a lag time of 1.54 ± 0.06 h and k_{app} of 1.52 ± 0.06 h^{-1}. Assembly kinetics in the presence of substoichiometric concentrations of N744 (4.1 μM) were not significantly different (lag time = 1.36 ± 0.07 h; k_{app} = 1.42 ± 0.07 h^{-1}). Moreover, the final equilibrium level of aggregation was unchanged confirming that N744 had little effect on Aβ_{1-40} assembly under these conditions.

The ability of N744 to modulate aggregation of α-synuclein, another protein that fibrillizes in response to anionic surfactants (*24*), was examined as well. On the basis of qualitative electron microscopy analysis, the presence of

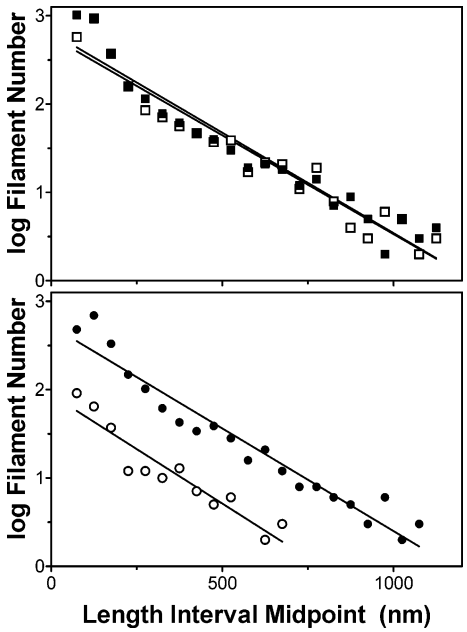

FIGURE 7: Length distribution of filaments during N744-mediated disaggregation. The relative length distributions of htau40 filaments ≥50 nm arising from the experiment shown in Figure 6 were calculated and plotted. Each data point represents the percentage of all filaments analyzed in four fields that segregated into consecutive length intervals (50 nm bins), whereas each line represents the best fit of the data points to an exponential distribution. At time 0 h (top), length distributions for treatment with DMSO vehicle control alone (■) and 4.7 μM N744 (□) were indistinguishable. Total filament length per field decreased over time, however, so that by 19 h (bottom) there were significantly fewer filaments in every bin of the N744-treated aliquot (○) relative to the DMSO only control (●). The maintenance of an exponential distribution with continually decreasing filament numbers is consistent with end-wise disaggregation of tau filaments and inconsistent with random filament breakage.

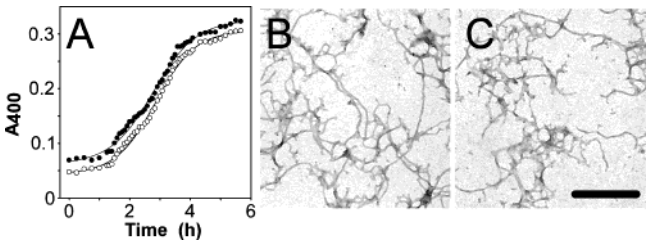

FIGURE 8: N744 is selective for tau fibrillization. (A) Aβ_{1-40} (20 μM) was incubated in assembly buffer in the presence of DMSO vehicle alone (○) or 4.1 μM N744 (●) and followed for 6 h by absorbance at 400 nm. Each point corresponds to absorbance at time *t*, whereas each solid line represents the best fit to an integral logistic equation. The close similarity in the two curves shows that N744 did not appreciably modulate the rate or extent of Aβ_{1-40} aggregation under these conditions. A second amyloid-forming protein, α-synuclein (5 μM), also was incubated (4 h at 37 °C) with 100 μM arachidonic acid in the presence of (B) DMSO vehicle or (C) 5 μM N744 and viewed by negative stain electron microscopy. N744 did not inhibit α-synuclein assembly under these conditions. Together, these data suggest that N744 is selective for tau protein when assayed at low micromolar concentrations. Bar = 500 nm.

N744 up to 10 μM did not modulate the fibrillization of 5 μM α-synuclein over a 4 h period (Figure 8). These data confirm that despite similarities in polymer structures (i.e., extended β-sheet) formed from different protein protomers, it is possible to select small ligands with target-selective inhibitory activity at low micromolar concentrations.

Scheme 1

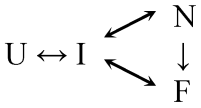

DISCUSSION

N744 is a potent inhibitor of inducer-mediated fibrillization of purified, recombinant htau40 and htau23. The pathway through which these isoforms fibrillize is not entirely clear, but at physiological concentrations in vitro it appears to parallel that of other amyloids by following the general Scheme 1 where U represents the unfolded state; I represents intermediate forms containing variable amounts of secondary structure; N represents the nucleus, the formation of which is rate limiting; and F represents filamentous forms, which again may be multiple and include protofilaments (*24*, *27*). Mature filaments eventually reach equilibrium with non-fibrillar protein, presumably in its U and/or I forms, which is reflected in the minimal concentration of protein required for assembly. Arachidonic acid accelerates this pathway by interacting with unfolded tau to yield anionic micelles upon which assembly competent intermediates rapidly form and stabilize (*13*, *20*). Nucleation follows intermediate formation in a time-dependent reaction, resulting in exponential distributions of filament lengths (*20*). A similar pathway appears to mediate arachidonic-acid induced α-synuclein fibrillization, resulting in shortened assembly lag times, increased apparent first-order rates of assembly, and decreased minimal concentrations at equilibrium relative to reactions conducted in the absence of micelles (*24*). Thus, N744 behaves as an arachidonic acid antagonist: it appears to inhibit filament formation and to raise the minimal concentration of assembly. The mechanism does not involve destabilization of micelles because N744 does not change fatty acid CMC and is active in reactions induced using anionic microspheres (which present stable anionic surfaces that do not vary with concentration).

Thus, N744 appears to interfere with steps in the tau fibrillization pathway. The ability of small molecules to antagonize amyloid fibril formation from other protein species has been reported previously (*36*−*40*), and it has been suggested these act at different stages of assembly to either lower the effective monomer concentration, block growth at filament ends, or increase the rate of filament breakage (*29*). In the case of globular proteins, inhibitors such as flufenamic acid acting on transthyretin or colchicine acting on tubulin can lead to substoichiometric inhibition of aggregation similar to that described here for tau protein (*41*, *42*). In the latter example, substoichiometric inhibition of aggregation and promotion of disassembly depends on filament polarity, where assembly and drug action occur primarily at one end while disassembly proceeds at the opposite end (*43*). Because tau filament elongation is unidirectional (*11*, *20*), this mechanism cannot be ruled out at present. But recombinant tau monomer is natively unfolded (*44*), making it unlikely that N744 could interact with tau in this way. Rather, an inhibitory mechanism for N744 is suggested by its structural similarity with Congo Red. Like N744, Congo Red is a planar aromatic dye, and on the basis of its binding stoichiometry and optical properties (birefrin-

gence), it is thought to bind all along the length of amyloid fibrils (*45*). However, Congo Red also binds globular proteins and the secondary structure elements of partially folded intermediates (*46*). Whereas arachidonic acid micelles appear to stabilize tau intermediates, binding of dye molecules may trap them and render them assembly incompetent, potentially diminishing filament nucleation. The relationship between filament nucleation rate and protein concentration has been proposed as

$$dC/dt = k_n(P_i)^n$$

where C is the number concentration of filaments, k_n is the nucleation rate constant, P_i is the concentration of the assembly competent species, and n is the number of molecules in the nucleus (*47*). Thus, small N744-mediated changes in the concentration of an assembly competent intermediate could have large, nonlinear effects on nucleation rate. The cooperative inhibition of tau filament nucleation with respect to N744 concentration (observed Hill coefficients between 1.6 and 1.8) may stem from this relationship. The apparent substoichiometric activity of N744 may stem from similar considerations because the concentration of intermediate is presumably lower than the total tau concentration in the reaction.

Inhibition of arachidonic acid-mediated nucleation appears to make a major contribution to N744 activity near the IC_{50} because the IC_{50}s for inhibition of total filament number and length were very similar. Consistent with this, filament length distributions skewed slightly toward longer filament lengths at low N744 concentrations. At concentrations approaching stoichiometry with total tau protomer, however, a shortening effect of N744 on filament length distributions became apparent. Moreover, treatment of mature filaments with stoichiometric concentrations of N744 led to filament diaggregation with first-order kinetics, maintenance of a near exponential distribution of filament lengths, and to steadily decreasing numbers of filaments. These characteristics were consistent with progressive endwise disaggregation and inconsistent with catastrophic filament breakage along the filament length (*30*). Together with N744-mediated decreases in filament length distributions, these data suggest that stoichiometric concentrations of N744 affect the equilibrium between fibrillar and nonfibrillar tau so that dissociation of tau from filament ends predominated. As a result of the new equilibrium, fibrillization of 4 μM htau40 was no longer supported.

The mechanism underlying these observations is not clear but is compatible with several scenarios involving changes in equilibrium at the growing filament end. First, trapping of intermediates with N744 could potentially decrease the amount of nonfibrillar tau available at equilibrium, resulting in decreased tau association at the growing filament end. This could occur from tau accumulating in assembly incompetent forms, including inhibitor-bound intermediates or competing, nonfibrillar conformations (*48*). Alternatively, if the intermediate itself is in equilibrium with the filament end (*27*), then N744 binding may render it assembly incompetent. The endwise disaggregation induced by N744 and the first order rate of approach to the new equilibrium is consistent with these models. Second, N744 may interact selectively and directly with filament ends, directly inhibiting monomer addition. Micelle and microsphere-mediated tau fibrillization is polar, so it is possible that the growing end may provide unique ligand-binding sites. A more detailed interpretation of N744 action on filament elongation will require clarification of the tau fibrillization pathway.

Partially folded intermediates appear to mediate fibrillization of several amyloid forming proteins (*27*, *49*, *50*). The structure of the intermediate could be a source of inhibitor selectivity. For example, anionic micelles accelerate fibrillization of both tau and α-synuclein at ~5 μM concentrations, but only tau intermediates fluoresce strongly in the presence of thioflavin dyes, suggesting that these intermediates differentially adopt beta-sheet structure (*11*, *24*). Similarly, N744 inhibits tau but not α-synuclein fibrillization at 5 μM concentration. Furthermore, Congo Red inhibits fibrillization of some proteins but not others (*40*). Characterization of assembly intermediates may yield insight into the structural basis of selectivity for ligands such as these and point the direction toward higher affinity and more selective fibrillization antagonists.

The close correlation between the spatial and the temporal distributions of neurofibrillary lesions and the severity of neuronal cell loss and dementia suggests a central role for tau fibrillization in the development of AD (*2*, *51*, *52*). This hypothesis has been greatly strengthened by the discovery of familial forms of neurofibrillary dementias that feature the development of neurofibrillary lesions in the absence of Aβ deposition and that are genetically linked to mutations in the tau gene (*53*, *54*). Yet whether tau fibrillization represents a toxic gain of function (i.e., a metabolic disruption or toxicity caused by the filaments themselves) or loss of function (i.e., interference with normal tau functions via the sequestration of tau into filaments) has not been established. Studies on the functional characteristics of tau mutants associated with familial neurofibrillary dementias are equivocal; while some of these mutants exhibit decreased microtubule binding in cell culture (*55*, *56*), they also exhibit an increased tendency to form filaments in vitro (*16*, *57*). The autosomal dominant mode of inheritance of most familial neurofibrillary dementias (*58*) suggests, but does not require, a gain of function mode of action, and it is possible that multiple tau-based mechanisms contribute to the neurodegeneration seen in the AD and the familial neurofibrillary dementias. A pharmacological approach to the problem using N744 could potentially clarify the contribution of tau fibrillization to neurodegeneration. Its substoichiometric mode of action suggests that inhibition of tau fibrillization will be feasible even at the high tau concentrations found associated with neuritic lesions (*59*).

On the basis of morphology and protomer stoichiometry, synthetic tau filaments induced by arachidonic acid treatment resemble straight filaments found early in disease (*60*) and correspond to one hemifilament of authentic PHF (*11*, *15*). The apparent commonality in protomer organization among these morphologies suggests that N744 may be useful for modulating tau fibrillization in various cell and animal models of tauopathic neurofibrillary degeneration.

REFERENCES

1. Buee, L., Bussiere, T., Buee-Scherrer, V., Delacourte, A., and Hof, P. R. (2000) Tau protein isoforms, phosphorylation and role in neurodegenerative disorders, *Brain. Res. Brain. Res. Rev. 33*, 95−130.

2. Braak, H., and Braak, E. (1991) Neuropathological stageing of Alzheimer-related changes, *Acta Neuropathol.* (*Berlin*) *82*, 239−259.
3. Braak, E., Braak, H., and Mandelkow, E. M. (1994) A sequence of cytoskeleton changes related to the formation of neurofibrillary tangles and neuropil threads, *Acta Neuropathol.* (*Berlin*) *87*, 554−567.
4. Feany, M. B., and Dickson, D. W. (1996) Neurodegenerative disorders with extensive tau pathology: a comparative study and review, *Ann. Neurol. 40*, 139−148.
5. Spillantini, M. G., Van Swieten, J. C., and Goedert, M. (2000) Tau gene mutations in frontotemporal dementia and parkinsonism linked to chromosome 17 (FTDP-17), *Neurogenetics 2*, 193−205.
6. Lewis, J., McGowan, E., Rockwood, J., Melrose, H., Nacharaju, P., Van Slegtenhorst, M., Gwinn-Hardy, K., Paul Murphy, M., Baker, M., Yu, X., Duff, K., Hardy, J., Corral, A., Lin, W. L., Yen, S. H., Dickson, D. W., Davies, P., and Hutton, M. (2000) Neurofibrillary tangles, amyotrophy, and progressive motor disturbance in mice expressing mutant (P301L) tau protein, *Nat. Genet. 25*, 402−405.
7. Gotz, J., Chen, F., Barmettler, R., and Nitsch, R. M. (2001) Tau filament formation in transgenic mice expressing P301L tau, *J. Biol. Chem. 276*, 529−534.
8. Hall, G. F., Chu, B., Lee, G., and Yao, J. (2000) Human tau filaments induce microtubule and synapse loss in an in vivo model of neurofibrillary degenerative disease, *J. Cell. Sci. 113*, 1373−1387.
9. Hall, G. F., Lee, V. M., Lee, G., and Yao, J. (2001) Staging of neurofibrillary degeneration caused by human tau overexpression in a unique cellular model of human tauopathy, *Am. J. Pathol. 158*, 235−246.
10. Hall, G. F., Chu, B., Lee, S., Liu, Y., and Yao, J. (2000) The single neurofilament subunit of the lamprey forms filaments and regulates axonal caliber and neuronal size in vivo, *Cell. Motil. Cytoskeleton. 46*, 166−182.
11. King, M. E., Ahuja, V., Binder, L. I., and Kuret, J. (1999) Ligand-dependent tau filament formation: implications for Alzheimer's disease progression, *Biochemistry 38*, 14851−14859.
12. Wilson, D. M., and Binder, L. I. (1997) Free fatty acids stimulate the polymerization of tau and amyloid beta peptides. In vitro evidence for a common effector of pathogenesis in Alzheimer's disease, *Am. J. Pathol. 150*, 2181−2195.
13. Chirita, C. N., Necula, M., and Kuret, J. (2003) Anionic Micelles and Vesicles Induce Tau Fibrillization in Vitro, *J. Biol. Chem. 278*, 25644−25650.
14. Barghorn, S., and Mandelkow, E. (2002) Toward a unified scheme for the aggregation of tau into Alzheimer paired helical filaments, *Biochemistry 41*, 14885−14896.
15. King, M. E., Ghoshal, N., Wall, J. S., Binder, L. I., and Ksiezak-Reding, H. (2001) Structural analysis of Pick's disease-derived and in vitro-assembled tau filaments, *Am. J. Pathol. 158*, 1481−1490.
16. Gamblin, T. C., King, M. E., Dawson, H., Vitek, M. P., Kuret, J., Berry, R. W., and Binder, L. I. (2000) In vitro polymerization of tau protein monitored by laser light scattering: method and application to the study of FTDP-17 mutants, *Biochemistry 39*, 6136−6144.
17. Abraha, A., Ghoshal, N., Gamblin, T. C., Cryns, V., Berry, R. W., Kuret, J., and Binder, L. I. (2000) C-terminal inhibition of tau assembly in vitro and in Alzheimer's disease, *J. Cell. Sci. 113*, 3737−3745.
18. Berriman, J., Serpell, L. C., Oberg, K. A., Fink, A. L., Goedert, M., and Crowther, R. A. (2003) Tau filaments from human brain and from in vitro assembly of recombinant protein show cross-beta structure, *Proc. Natl. Acad. Sci. U.S.A. 100*, 9034−9038.
19. von Bergen, M., Friedhoff, P., Biernat, J., Heberle, J., Mandelkow, E. M., and Mandelkow, E. (2000) Assembly of tau protein into Alzheimer paired helical filaments depends on a local sequence motif ((306)VQIVYK(311)) forming beta structure, *Proc. Natl. Acad. Sci. U.S.A. 97*, 5129−5134.
20. Chirita, C. N., and Kuret, J. (2004) Evidence for an intermediate in tau filament formation, *Biochemistry 43*, in press.
21. Wischik, C. M., Edwards, P. C., Lai, R. Y., Roth, M., and Harrington, C. R. (1996) Selective inhibition of Alzheimer disease-like tau aggregation by phenothiazines, *Proc. Natl. Acad. Sci. U.S.A. 93*, 11213−11218.
22. Carmel, G., Mager, E. M., Binder, L. I., and Kuret, J. (1996) The structural basis of monoclonal antibody Alz50's selectivity for Alzheimer's disease pathology, *J. Biol. Chem. 271*, 32789−32795.
23. King, M. E., Gamblin, T. C., Kuret, J., and Binder, L. I. (2000) Differential assembly of human tau isoforms in the presence of arachidonic acid, *J. Neurochem. 74*, 1749−1757.
24. Necula, M., Chirita, C. N., and Kuret, J. (2003) Rapid anionic micelle-mediated alpha-synuclein fibrillization in vitro, *J. Biol. Chem. 278*, 46674−46680.
25. Snyder, S. W., Ladror, U. S., Wade, W. S., Wang, G. T., Barrett, L. W., Matayoshi, E. D., Huffaker, H. J., Krafft, G. A., and Holzman, T. F. (1994) Amyloid-beta aggregation: selective inhibition of aggregation in mixtures of amyloid with different chain lengths, *Biophys. J. 67*, 1216−1228.
26. Evans, K. C., Berger, E. P., Cho, C. G., Weisgraber, K. H., and Lansbury, P. T., Jr. (1995) Apolipoprotein E is a kinetic but not a thermodynamic inhibitor of amyloid formation: implications for the pathogenesis and treatment of Alzheimer's disease, *Proc. Natl. Acad. Sci. U.S.A. 92*, 763−767.
27. Uversky, V. N., Li, J., and Fink, A. L. (2001) Evidence for a partially folded intermediate in alpha-synuclein fibril formation, *J. Biol. Chem. 276*, 10737−10744.
28. Goedert, M., Spillantini, M. G., Jakes, R., Rutherford, D., and Crowther, R. A. (1989) Multiple isoforms of human microtubule-associated protein tau: sequences and localization in neurofibrillary tangles of Alzheimer's disease, *Neuron 3*, 519−526.
29. Masel, J., and Jansen, V. A. (2000) Designing drugs to stop the formation of prion aggregates and other amyloids, *Biophys. Chem. 88*, 47−59.
30. Kristofferson, D., Karr, T. L., and Purich, D. L. (1980) Dynamics of linear protein polymer disassembly, *J. Biol. Chem. 255*, 8567−8572.
31. Wilson, D. M., and Binder, L. I. (1995) Polymerization of microtubule-associated protein tau under near-physiological conditions, *J. Biol. Chem. 270*, 24306−24314.
32. Gamblin, T. C., King, M. E., Kuret, J., Berry, R. W., and Binder, L. I. (2000) Oxidative regulation of fatty acid-induced tau polymerization, *Biochemistry 39*, 14203−14210.
33. Briehl, R. W., Mann, E. S., and Josephs, R. (1990) Length distributions of hemoglobin S fibers, *J. Mol. Biol. 211*, 693−698.
34. Agarwal, G., Wang, J. C., Kwong, S., Cohen, S. M., Ferrone, F. A., Josephs, R., and Briehl, R. W. (2002) Sickle hemoglobin fibers: mechanisms of depolymerization, *J. Mol. Biol. 322*, 395−412.
35. Caprathe, B. W., Gilmore, J. L., Hays, S. J., Jaen, J. C., and LeVine, H. (1999), U.S. Patent 6 001 331.
36. Heiser, V., Engemann, S., Brocker, W., Dunkel, I., Boeddrich, A., Waelter, S., Nordhoff, E., Lurz, R., Schugardt, N., Rautenberg, S., Herhaus, C., Barnickel, G., Bottcher, H., Lehrach, H., and Wanker, E. E. (2002) Identification of benzothiazoles as potential polyglutamine aggregation inhibitors of Huntington's disease by using an automated filter retardation assay, *Proc. Natl. Acad. Sci. U.S.A. 99*, 16400−16406.
37. Kuner, P., Bohrmann, B., Tjernberg, L. O., Naslund, J., Huber, G., Celenk, S., Gruninger-Leitch, F., Richards, J. G., Jakob-Roetne, R., Kemp, J. A., and Nordstedt, C. (2000) Controlling polymerization of beta-amyloid and prion-derived peptides with synthetic small molecule ligands, *J. Biol. Chem. 275*, 1673−1678.
38. Lashuel, H. A., Hartley, D. M., Balakhaneh, D., Aggarwal, A., Teichberg, S., and Callaway, D. J. (2002) New class of inhibitors of amyloid-beta fibril formation. Implications for the mechanism of pathogenesis in Alzheimer's disease, *J. Biol. Chem. 277*, 42881−42890.
39. Rudyk, H., Vasiljevic, S., Hennion, R. M., Birkett, C. R., Hope, J., and Gilbert, I. H. (2000) Screening Congo Red and its analogues for their ability to prevent the formation of PrP-res in scrapie-infected cells, *J. Gen. Virol. 81*, 1155−1164.
40. Lorenzo, A., and Yankner, B. A. (1994) Beta-amyloid neurotoxicity requires fibril formation and is inhibited by Congo Red, *Proc. Natl. Acad. Sci. U.S.A. 91*, 12243−12247.
41. Peterson, S. A., Klabunde, T., Lashuel, H. A., Purkey, H., Sacchettini, J. C., and Kelly, J. W. (1998) Inhibiting transthyretin conformational changes that lead to amyloid fibril formation, *Proc. Natl. Acad. Sci. U.S.A. 95*, 12956−12960.
42. Skoufias, D. A., and Wilson, L. (1992) Mechanism of inhibition of microtubule polymerization by colchicine: inhibitory potencies of unliganded colchicine and tubulin−colchicine complexes, *Biochemistry 31*, 738−746.
43. Perez-Ramirez, B., Andreu, J. M., Gorbunoff, M. J., and Timasheff, S. N. (1996) Stoichiometric and substoichiometric inhibition of tubulin self-assembly by colchicine analogues, *Biochemistry 35*, 3277−3285.

44. Schweers, O., Schonbrunn-Hanebeck, E., Marx, A., and Mandelkow, E. (1994) Structural studies of tau protein and Alzheimer paired helical filaments show no evidence for beta structure, *J. Biol. Chem. 269*, 24290−24297.
45. Klunk, W. E., Pettegrew, J. W., and Abraham, D. J. (1989) Quantitative evaluation of congo red binding to amyloid-like proteins with a beta-pleated sheet conformation, *J. Histochem. Cytochem. 37*, 1273−1281.
46. Khurana, R., Uversky, V. N., Nielsen, L., and Fink, A. L. (2001) Is Congo red an amyloid-specific dye? *J. Biol. Chem. 276*, 22715−22721.
47. Tobacman, L. S., and Korn, E. D. (1983) The kinetics of actin nucleation and polymerization, *J. Biol. Chem. 258*, 3207−3214.
48. Pertinhez, T. A., Bouchard, M., Smith, R. A. G., Dobson, C. M., and Smith, L. J. (2002) Stimulation and inhibition of fibril formation by a peptide in the presence of different concentrations of SDS, *FEBS Lett. 529*, 193−197.
49. Ahmad, A., Millett, I. S., Doniach, S., Uversky, V. N., and Fink, A. L. (2003) Partially folded intermediates in insulin fibrillation, *Biochemistry 42*, 11404−11416.
50. Khurana, R., Gillespie, J. R., Talapatra, A., Minert, L. J., Ionescu-Zanetti, C., Millett, I., and Fink, A. L. (2001) Partially folded intermediates as critical precursors of light chain amyloid fibrils and amorphous aggregates, *Biochemistry 40*, 3525−3535.
51. Gomez-Isla, T., Price, J. L., McKeel, D. W., Jr., Morris, J. C., Growdon, J. H., and Hyman, B. T. (1996) Profound loss of layer II entorhinal cortex neurons occurs in very mild Alzheimer's disease, *J. Neurosci. 16*, 4491−4500.
52. Ghoshal, N., Garcia-Sierra, F., Wuu, J., Leurgans, S., Bennett, D. A., Berry, R. W., and Binder, L. I. (2002) Tau conformational changes correspond to impairments of episodic memory in mild cognitive impairment and Alzheimer's disease, *Exp. Neurol. 177*, 475−493.
53. Spillantini, M. G., Murrell, J. R., Goedert, M., Farlow, M. R., Klug, A., and Ghetti, B. (1998) Mutation in the tau gene in familial multiple system tauopathy with presenile dementia, *Proc. Natl. Acad. Sci. U.S.A. 95*, 7737−7741.
54. Hutton, M., Lendon, C. L., Rizzu, P., Baker, M., Froelich, S., Houlden, H., Pickering-Brown, S., Chakraverty, S., Isaacs, A., Grover, A., Hackett, J., Adamson, J., Lincoln, S., Dickson, D., Davies, P., Petersen, R. C., Stevens, M., de Graaff, E., Wauters, E., van Baren, J., Hillebrand, M., Joosse, M., Kwon, J. M., Nowotny, P., Heutink, P. et al. (1998) Association of missense and 5′-splice-site mutations in tau with the inherited dementia FTDP-17, *Nature 393*, 702−705.
55. Hasegawa, M., Smith, M. J., and Goedert, M. (1998) Tau proteins with FTDP-17 mutations have a reduced ability to promote microtubule assembly, *FEBS Lett 437*, 207−210.
56. Hong, M., Zhukareva, V., Vogelsberg-Ragaglia, V., Wszolek, Z., Reed, L., Miller, B. I., Geschwind, D. H., Bird, T. D., McKeel, D., Goate, A., Morris, J. C., Wilhelmsen, K. C., Schellenberg, G. D., Trojanowski, J. Q., and Lee, V. M. (1998) Mutation-specific functional impairments in distinct tau isoforms of hereditary FTDP-17, *Science 282*, 1914−1917.
57. Goedert, M., Jakes, R., and Crowther, R. A. (1999) Effects of frontotemporal dementia FTDP-17 mutations on heparin-induced assembly of tau filaments, *FEBS Lett 450*, 306−311.
58. Reed, L. A., Schmidt, M. L., Wszolek, Z. K., Balin, B. J., Soontornniyomkij, V., Lee, V. M., Trojanowski, J. Q., and Schelper, R. L. (1998) The neuropathology of a chromosome 17-linked autosomal dominant parkinsonism and dementia (pallido-ponto-nigral degeneration), *J. Neuropathol. Exp. Neurol. 57*, 588−601.
59. Khatoon, S., Grundke-Iqbal, I., and Iqbal, K. (1992) Brain levels of microtubule-associated protein tau are elevated in Alzheimer's disease: a radioimmuno-slot-blot assay for nanograms of the protein, *J. Neurochem. 59*, 750−753.
60. Perry, G., Kawai, M., Tabaton, M., Onorato, M., Mulvihill, P., Richey, P., Morandi, A., Connolly, J. A., and Gambetti, P. (1991) Neuropil threads of Alzheimer's disease show a marked alteration of the normal cytoskeleton, *J. Neurosci. 11*, 1748−1755.

BI036094H